Supporting Information

# Large-diameter and Heteroatom-doped Graphene Nanotubes Decorated with Transition Metals as Carbon Hosts for Lithium-Sulfur Batteries

Ogechi Ogoke[a,1], Sooyeon Hwang[b,1], Benjamin Hultman[a], Mengjie Chen[a,], Stavros Karakalos[c] Yanghua He[a], , Adam Ramsey[a], Dong Su[b,*] ,Paschalis Alexandridis[a,*], and Gang Wu[a,*]

[a]Department of Chemical and Biological Engineering, University at Buffalo, The State University of New York, Buffalo, NY 14260, United States
Email: gangwu@buffalo.edu (G. Wu) and palexand@buffalo.edu (P. Alexandridis)

[b]Center for Functional Nanomaterials, Brookhaven National Laboratory, Upton, NY 11973, United States
Email: dsu@bnl.gov (D. Su)

[c]Department of Chemical Engineering, University of South Carolina, Columbia, SC 29208, United States

[1], These authors contributed equally

**Figures S1 to S16**

**Tables S1 to S2**

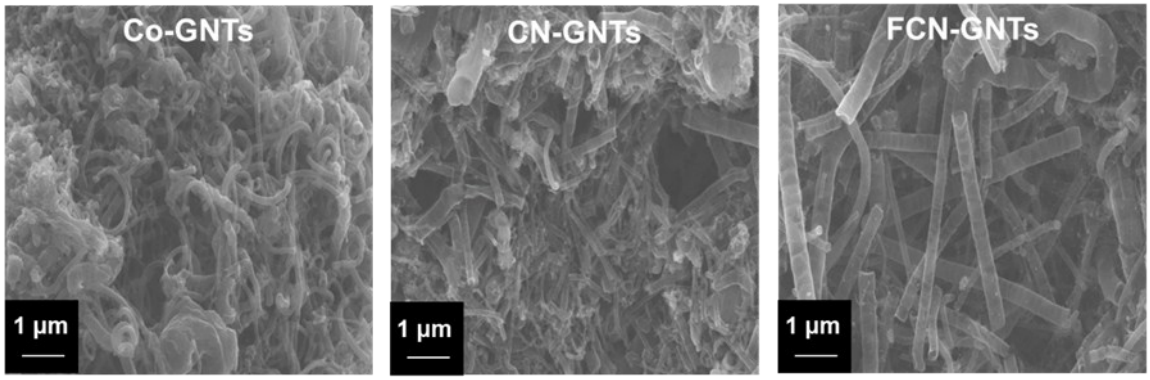


**Figure S1**. SEM images of each heteroatom doped graphene nanotube samples. Cobalt doped graphene nanotubes (CO-GNTs), cobalt-nickel doped graphene nanotubes (CN-GNTs), and iron-cobalt-nickel doped graphene nanotubes (FCN-GNTs) respectively.

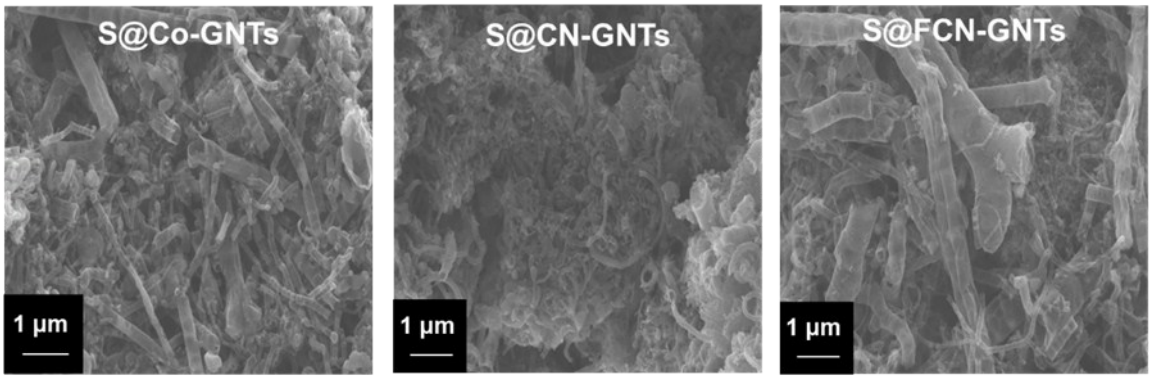


**Figure S2**. SEM images of sulfur infused heteroatom doped graphene nanotube samples. Sulfur infused cobalt-nickel doped graphene nanotubes S@CO-GNTs, sulfur infused cobalt-nickel doped graphene nanotubes S@CN-GNTs, and sulfur infused iron-cobalt-nickel doped graphene nanotubes S@FCN-GNTs

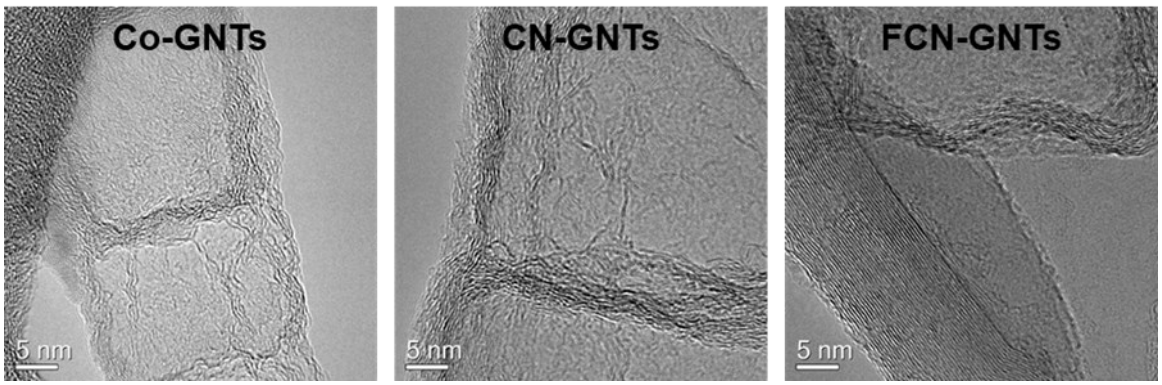


**Figure S3**. HRTEM images of Co-GNTs, CN-GNTs, and FCN-GNTs. The scale bars are 5 nm.

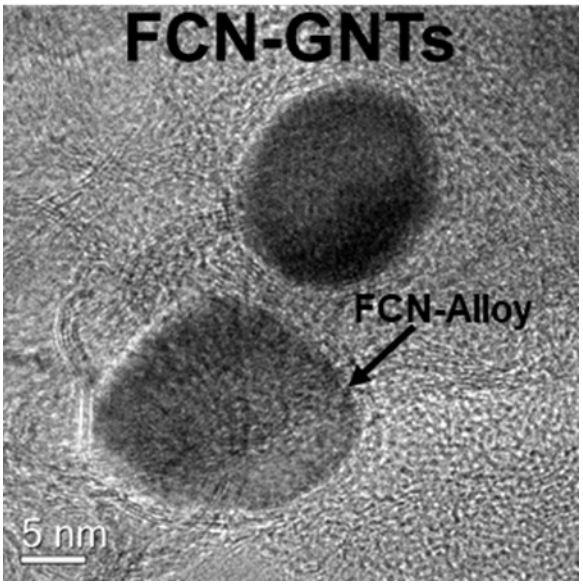


**Figure S4**. HRTEM image of the FCN-alloy decorated graphene nanotubes (FCN-GNTs). The particle size is roughly 10-20 nm. The scale bar is 5 nm.

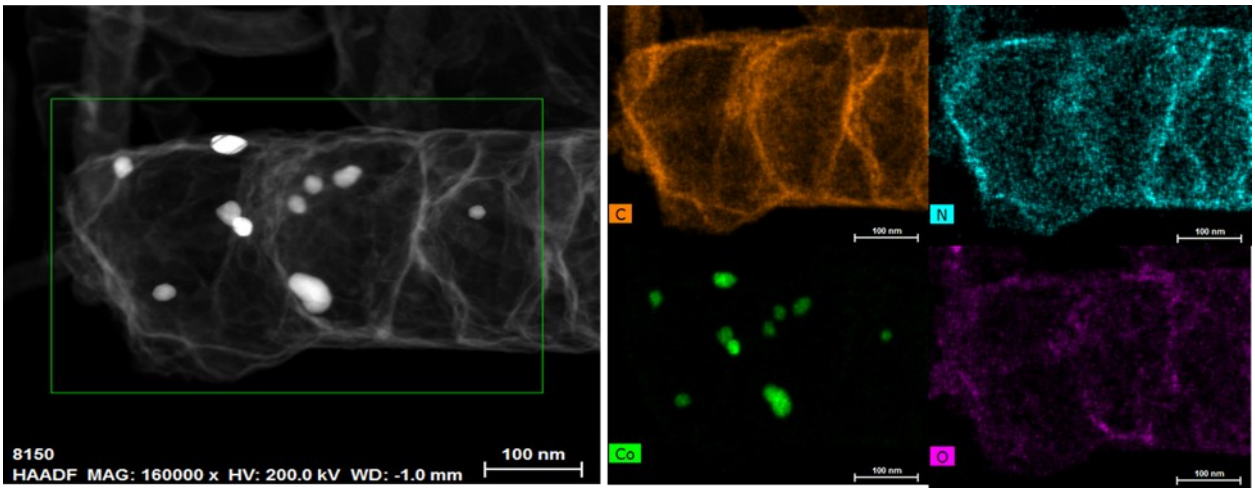


**Figure S5**. STEM and elemental mapping for Co-GNTs, showing uniform nitrogen doping and decorated Co particles.

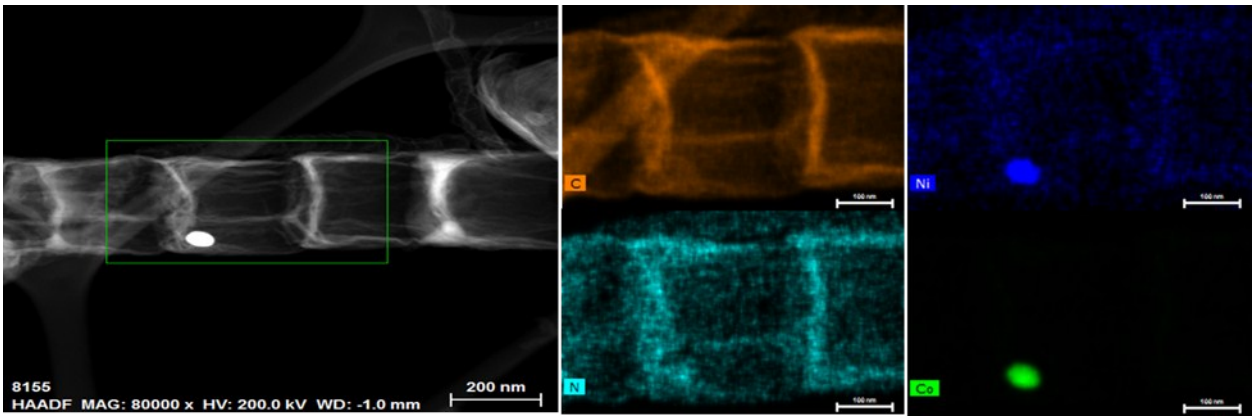


**Figure S6**. STEM and elemental mapping for CoNi-GNTs, showing uniform nitrogen doping and decorated CoNi alloy particles.

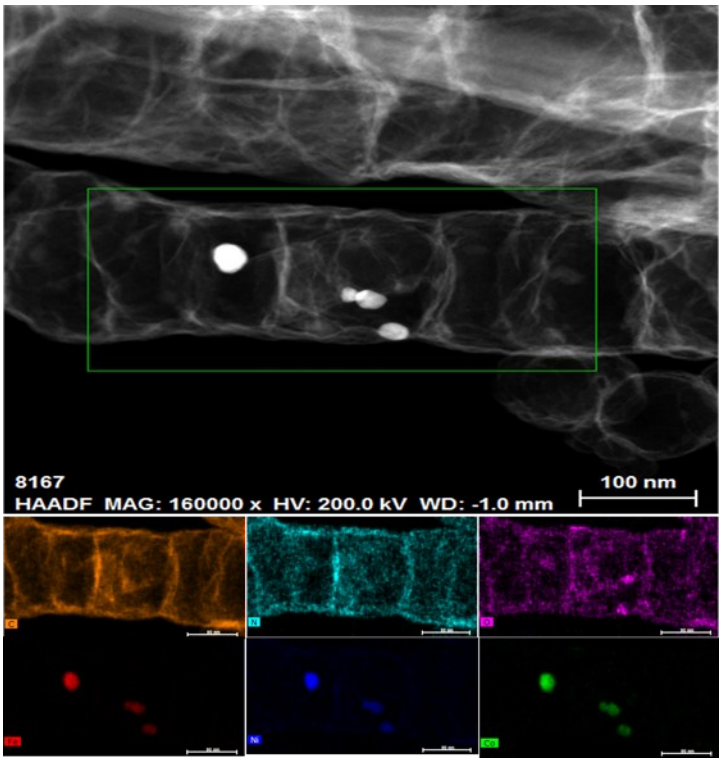


**Figure S7**. STEM and elemental mapping for FeCoNi-GNTs, showing uniform nitrogen doping and decorated FeCoNi alloy particles.

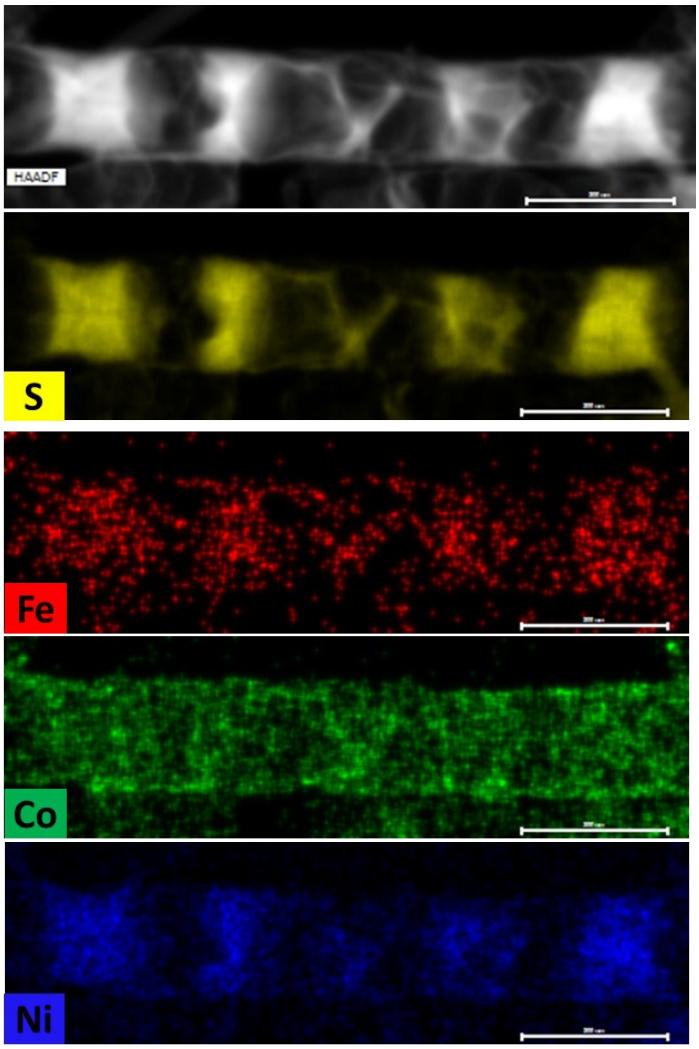


**Figure S8**. Atomically dispersed atomic metal sites in graphene tubes, which are likely associated with adsorbed S.

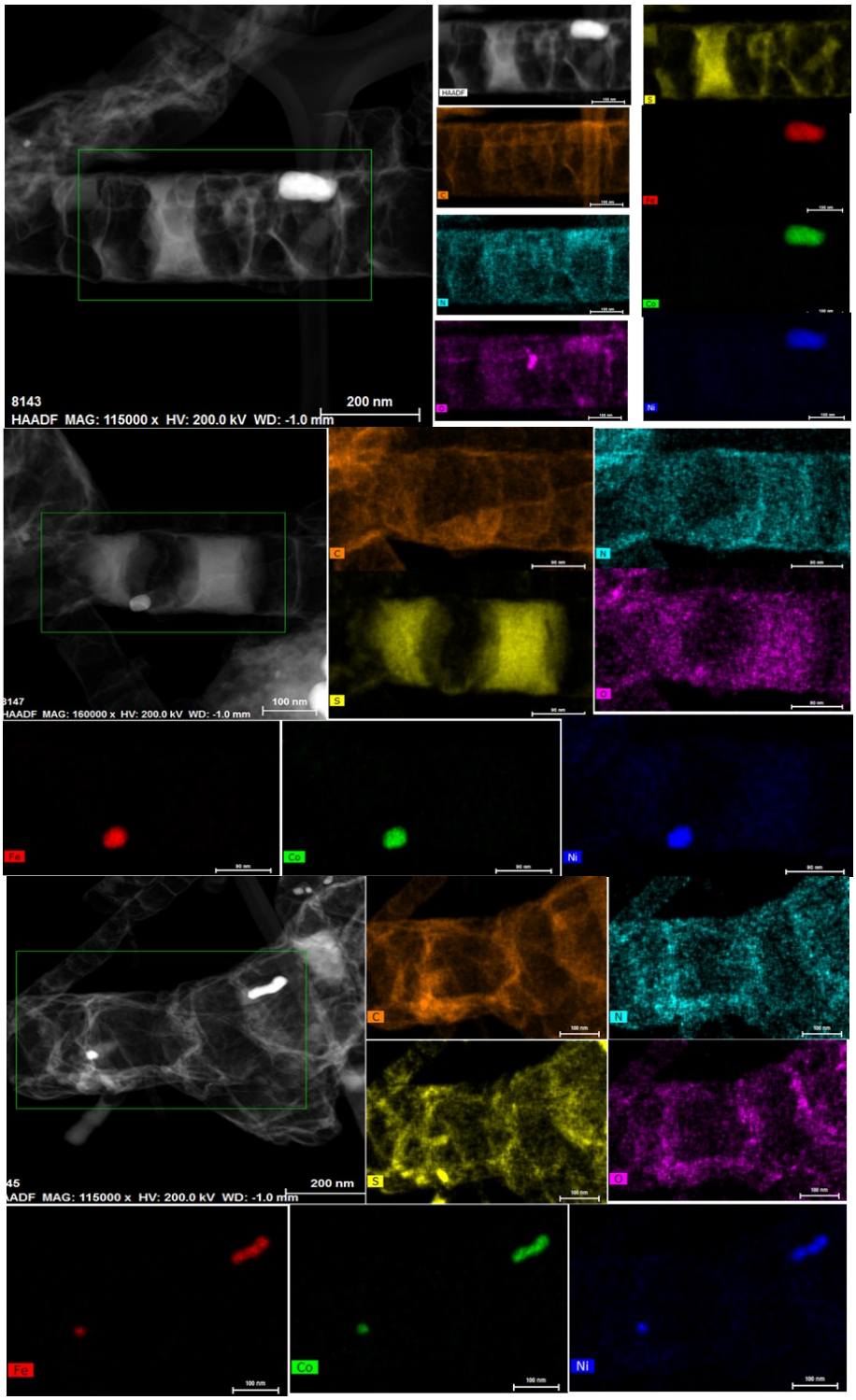


**Figure S9**. STEM and elemental EDX mapping for S@FeCoNi-GNTs containing S inside the tubes. The green line highlighted region is elementally analyzed. The carbon (orange) tube-structure is visible with N (turquoise) and O (pink) doping present throughout. Sulfur (yellow) has

diffused, via melting, into the tube-structure which allows for excellent contact with the carbon hosts structure.

**Table S1**. Representative elemental content for the S@FeCoNi-GNT carbon. The actual ratios among F, Co, and Ni are close to the nominated 1: 1: 1

| | Atomic % |
|---|---|
| Fe | 0.37 |
| Co | 0.55 |
| Ni | 0.68 |
| C | 72.81 |
| N | 4.69 |
| O | 3.01 |
| S | 17.88 |

| | Atomic % |
|---|---|
| Fe | 23.17 |
| Co | 34.31 |
| Ni | 42.52 |

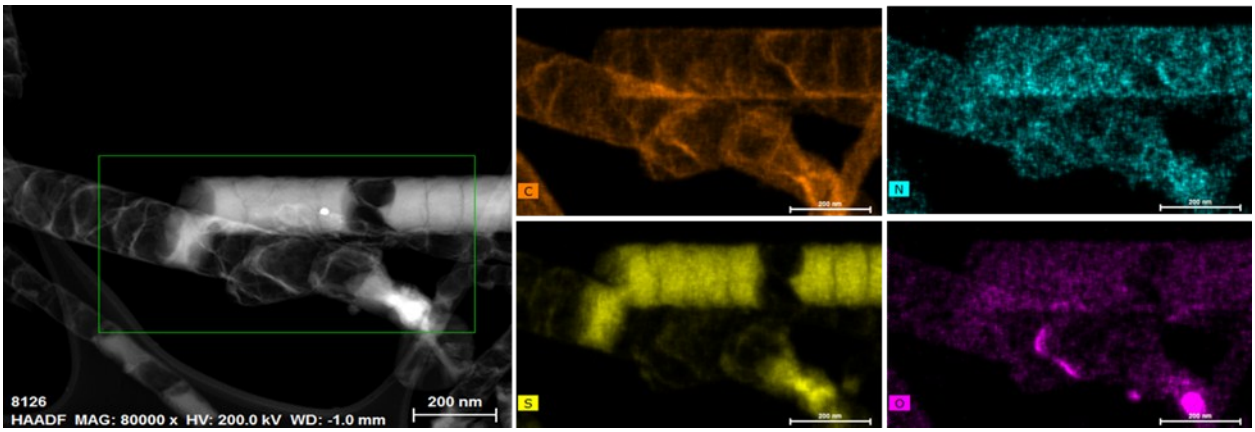


**Figure S10**. STEM and elemental EDX mapping for S@Co-GNTs containing S inside the tubes. The green line highlighted region is elementally analyzed. The carbon (orange) tube-structure is visible with N (turquoise) and O (pink) doping present throughout. Sulfur (yellow) has diffused, via melting, into the tube-structure which allows for excellent contact with the carbon hosts structure.

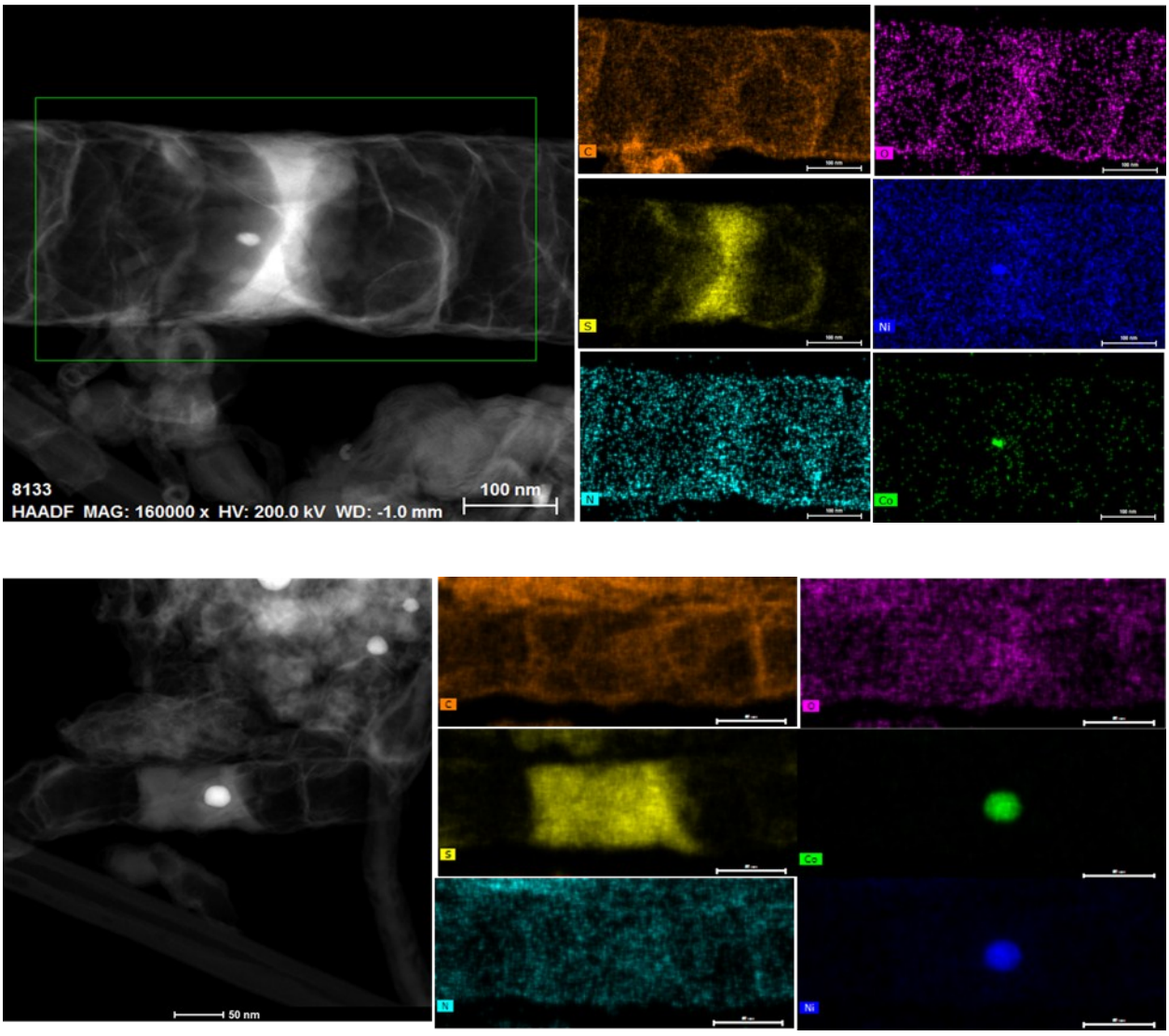


**Figure S11**. STEM and elemental EDX mapping for S@CoNi-GNTs containing S inside the tubes. The green line highlighted region is elementally analyzed. The carbon (orange) tube-structure is visible with N (turquoise) and O (pink) doping present throughout. Sulfur (yellow) has diffused, via melting, into the tube-structure which allows for excellent contact with the carbon hosts structure.

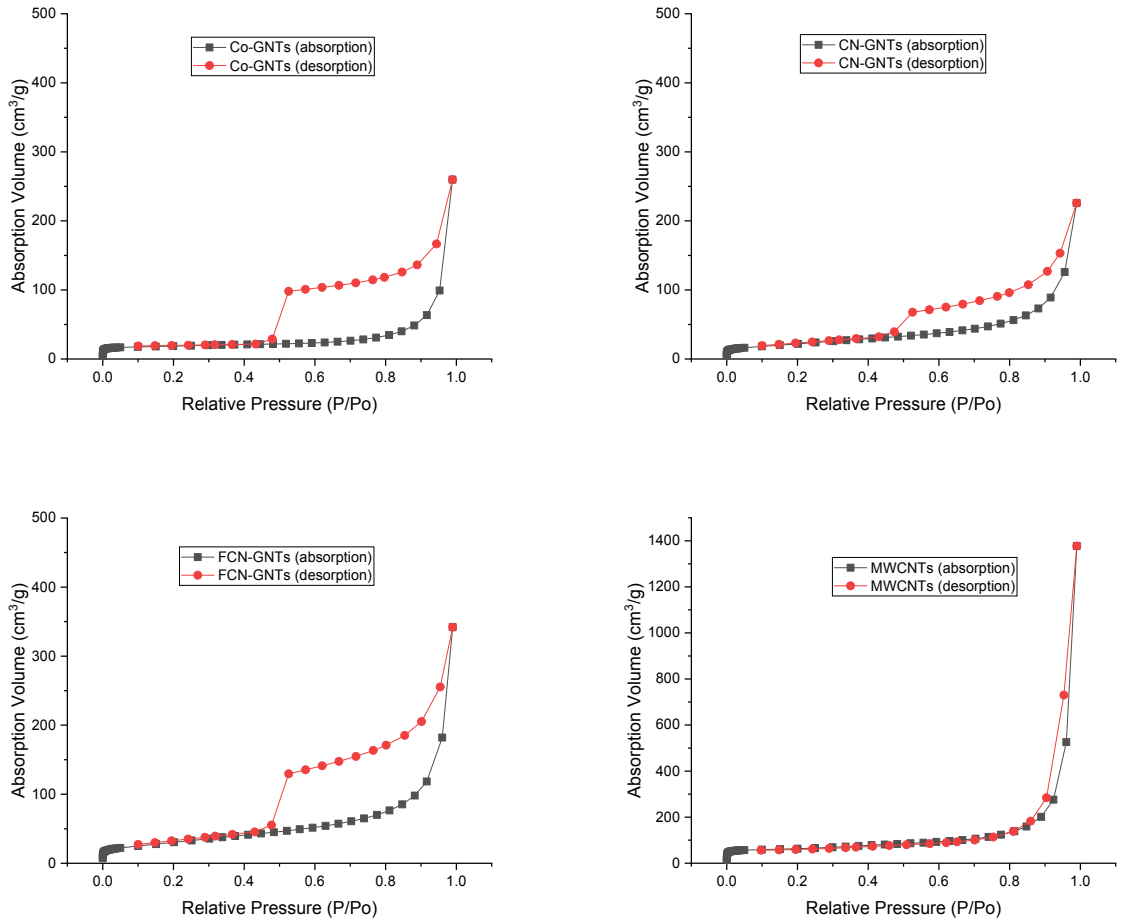


**Figure S12**. The $N_2$ adsorption and desorption isotherms of Co-GNTs, CN-GNTs, FCN-GNTs, and MWCNTs.

**Table S2**. Elemental qualification of M-GNTs determined by XPS.

| at.% | C | N | O | Co | Ni | Fe |
|---|---|---|---|---|---|---|
| Co-GNT | 93.8 | 4.1 | 1.6 | 0.5 | - | - |
| CoNi-GNT | 92.9 | 4.5 | 1.5 | 0.3 | 0.8 | - |
| FeCoNi-GNT | 91.8 | 5.4 | 1.6 | 0.3 | 0.8 | 0.1 |

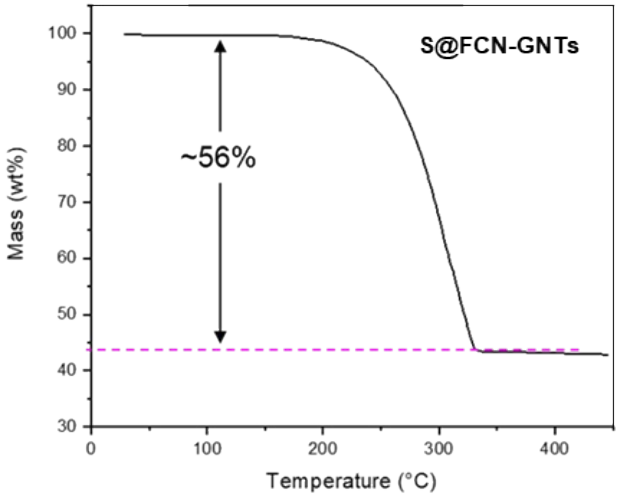


**Figure S13**. TGA of the S@FCN-GNTs material.

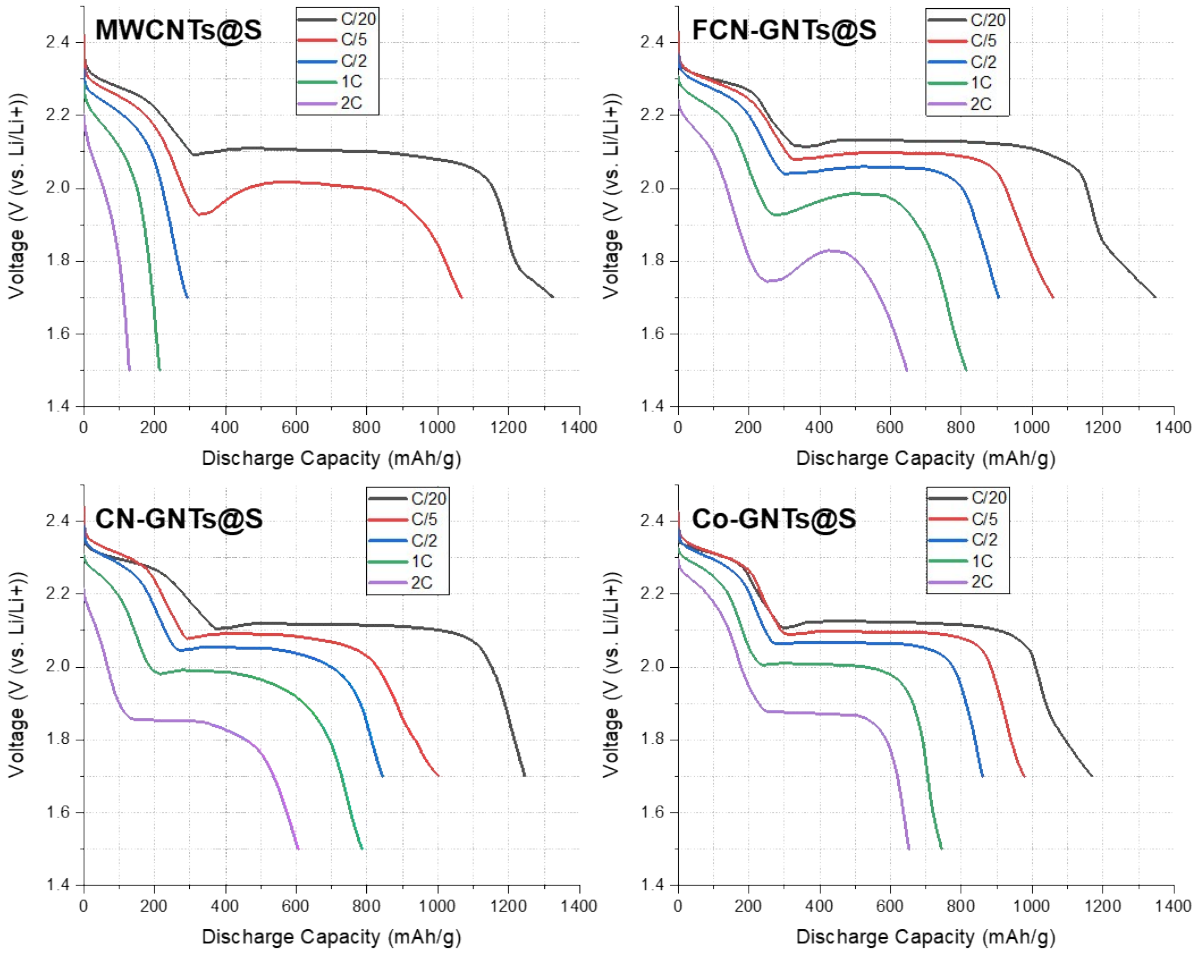


**Figure S14**. The C/20, C/5, C/2, 1C, and 2C voltage profiles of S@MWCNTs, S@Co-GNTs, S@CN-GNTs, and S@FCN-GNTs.

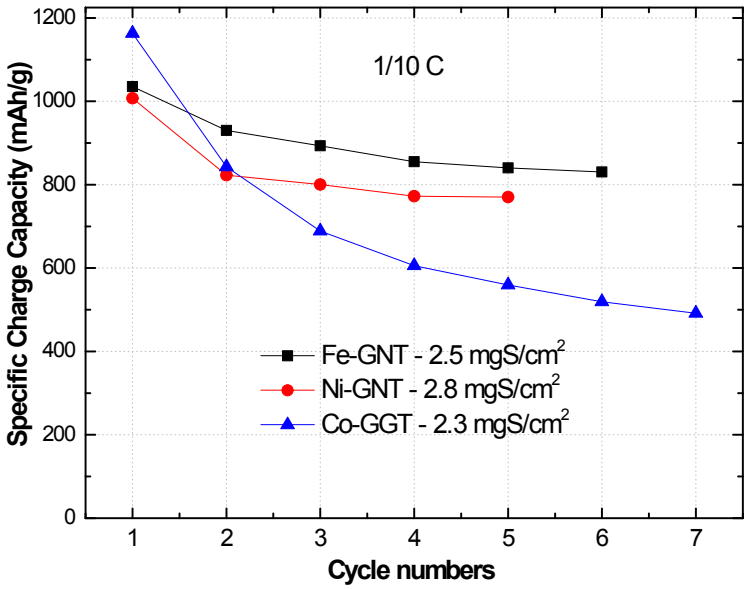


**Figure S15**. Short-term cyclic stability of M-GNT hosted S cathodes in Li-S batteries

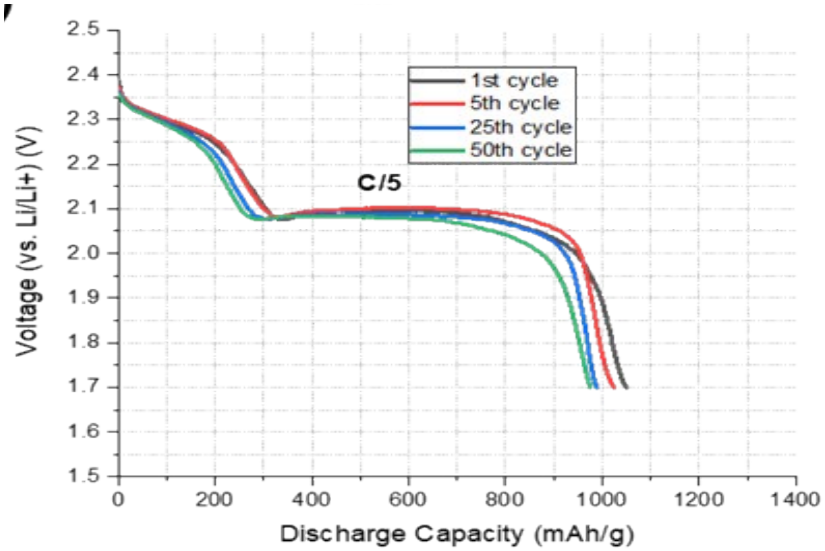


**Figure S16**. Discharge voltage profiles of 1st, 5th, 25th, and 50th cycles for S@FeCoNi-GNTs cells at C/5.

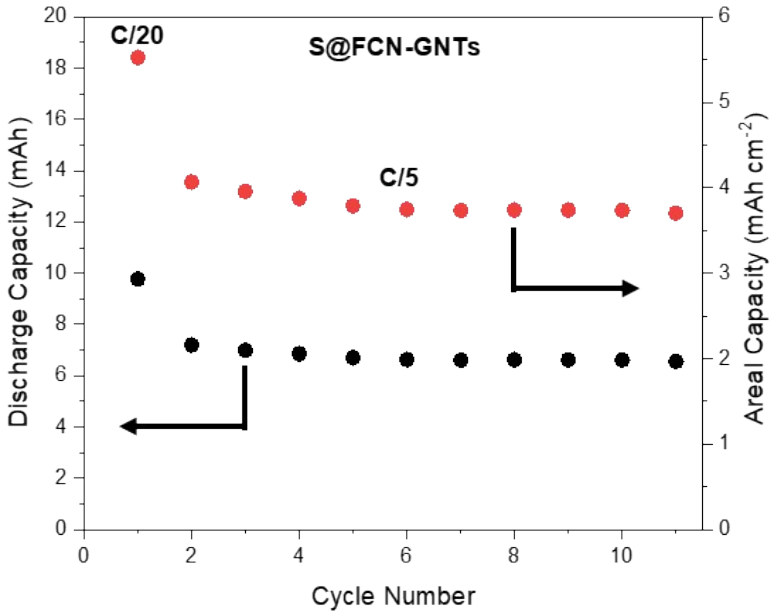


**Figure S17.** Cycle tests in specific capacity and areal capacity of ultra-high loading S@FCN-GNTs (~4.5 mgS $cm^{-2}$), which discharged 1234.7 mAh $g^{-1}$ (5.52 mAh $cm^{-2}$) at C/20 and 909.0 mAh $g^{-1}$ (4.07 mAh $cm^{-2}$) at C/5.

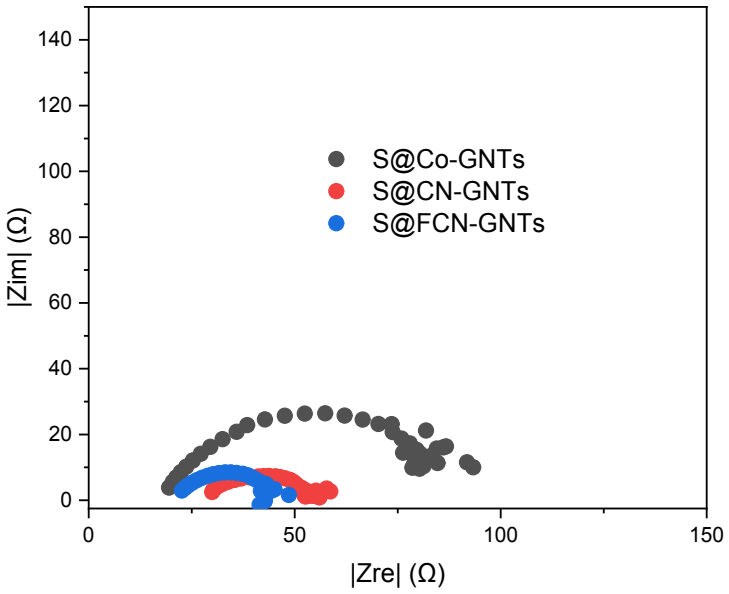


**Figure S18**. EIS of full Li-S cells with S@Co-GNTs, S@CN-GNTs, and S@FCN-GNTs materials after rate capability testing from 1.0 Hz to 100 kHz.

**Table S3**. A comparison of the S@FCN-GNTs material's cycle lifetime performance at 1C (this work) to other heteroatom-doped carbon nanostructures for Li-S batteries reported in the literature. (* = 1600 mA $g^{-1}$)

| Carbon Morphology | Doped Heteroatoms and Nanoparticles | Voltage Range (V) | Initial Performance at 1C (mAh $g^{-1}$) | After (n) Cycles at 1C (mAh $g^{-1}$) | Capacity loss per cycle (%) |
|---|---|---|---|---|---|
| **This work (S@FCN-GNTs)** | **N/O and Fe, Co, and Ni** | **2.7 – 1.5** | **956** | **554 (500)** | **0.0839** |
| Carbon nanosheets[1] | N and Co | 2.8 – 1.7 | 825 | 633 (200) | 0.0960 |
| Carbon microclusters[2] | N and Co | 2.8 – 1.7 | 905 | 650 (400) | 0.0704 |
| Hierarchical porous carbon[3] | N/P | 2.8 – 1.7 | 614 | 456 (500) | 0.0514 |
| Nonporous carbon[4] | N/O | 3.0 – 1.5 | 360* | 540 (300)* | --- |

**References:**


1. S. Liu, J. Li, X. Yan, Q. Su, Y. Lu, J. Qiu, Z. Wang, X. Lin, J. Huang and R. Liu, *Advanced Materials*, 2018, **30**, 1706895.
2. P. Wang, Z. Zhang, X. Yan, M. Xu, Y. Chen, J. Li, J. Li, K. Zhang and Y. Lai, *Journal of Materials Chemistry A*, 2018, **6**, 14178-14187.
3. J. Cai, C. Wu, Y. Zhu, K. Zhang and P. K. Shen, *Journal of Power Sources*, 2017, **341**, 165-174.
4. K. Mi, S. Chen, B. Xi, S. Kai, Y. Jiang, J. Feng, Y. Qian and S. Xiong, *Advanced Functional Materials*, 2017, **27**, 1604265.